REPORT DOCUMENTATION PAGE

Form Approved
OMB No. 0704-0188

1. REPORT DATE *(DD-MM-YYYY)*	2. REPORT TYPE	3. DATES COVERED *(From - To)*
07/22/2011	Final Technical	5/1/2008 to 4/30/2011

4. TITLE AND SUBTITLE
Sensitive Detection Using Microfluidics and Nonlinear Amplification

5a. CONTRACT NUMBER

5b. GRANT NUMBER
N00014-08-1-0936

5c. PROGRAM ELEMENT NUMBER

6. AUTHOR(S)
Rustem F. Ismagilov

5d. PROJECT NUMBER

5e. TASK NUMBER

5f. WORK UNIT NUMBER

7. PERFORMING ORGANIZATION NAME(S) AND ADDRESS(ES)
The University of Chicago
Office of Sponsored Programs
6030 S Ellis Ave.
Chicago, IL 60637

8. PERFORMING ORGANIZATION REPORT NUMBER
5-28365; FP039499-01-PR

9. SPONSORING/MONITORING AGENCY NAME(S) AND ADDRESS(ES)
Office of Naval Research
230 S. Dearborn
Room 380
Chicago, IL 60604-1595

10. SPONSOR/MONITOR'S ACRONYM(S)
ONR

11. SPONSOR/MONITOR'S REPORT NUMBER(S)

12. DISTRIBUTION/AVAILABILITY STATEMENT
Approved for Public Release; distribution is Unlimited

13. SUPPLEMENTARY NOTES

14. ABSTRACT
Rapid detection of small particles such as pathogens, environmental pollutants, and microorganisms is important for both the security and health of society at large. The main goal of this proposal is to establish the scientific foundations for rapidly detecting small particles at low concentrations by combining controlled chemical autocatalytic amplification and stochastic confinement of small particles with the microfluidic expertise that has been developed in PI's laboratories. We focus on developing computational models to predict the optimal single step amplification and multi-step amplification cascades, and we will compare these models to existing biological amplification networks, including blood clotting and apoptosis. Simultan

15. SUBJECT TERMS

16. SECURITY CLASSIFICATION OF:			17. LIMITATION OF ABSTRACT	18. NUMBER OF PAGES	19a. NAME OF RESPONSIBLE PERSON
a. REPORT	b. ABSTRACT	c. THIS PAGE			Rustem Ismagilov
U	U	U	U		19b. TELEPHONE NUMBER *(Include area code)* 773-702-5816

RESEARCH FINDINGS:

This research uses a simple experimental chemical model to understand the nonlinear dynamics of the complex biochemical network of hemostasis (blood clotting). The chemical model is based on a modular mechanism describing initiation of clotting. Briefly, we constructed a chemical model of the hemostasis network, which contains approximately 80 reactions. Our model contained three interacting modules; each module consisted of a single chemical reaction with appropriate kinetics. In the model, a threshold response was regulated by the interaction of the three modules. Previously published work describes this approach in detail (*PNAS* **2006** 103:15747-15752). Using this model system, we demonstrated that the spatial localization of bacteria profoundly affected coagulation of human and mouse blood and plasma.

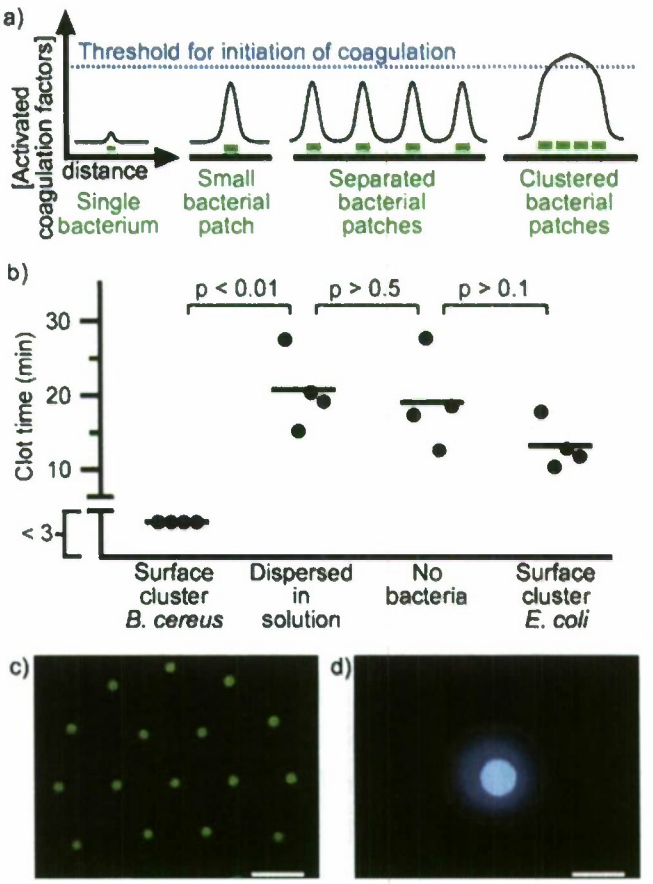

Figure 1. Human blood plasma coagulates on spatially localized B. cereus. (a) A schematic drawing illustrates the coagulation potential of a single bacterium, a single small surface patch of bacteria, surface patches of bacteria that are separated, and surface patches of bacteria that are clustered together. (b) A chart compares the clotting times of human blood plasma on the same amount of bacteria either clustered in a large patch or dispersed in solution. (c and d) Fluorescent photographs of a microfluidic chamber used to test coagulation (blue fluorescence) of human blood plasma on clustered bacteria (green fluorescence) patterned as patches of different sizes. Coagulation occurs rapidly on a large patch (d), but not on an array of smaller patches containing the same amount of bacteria (c).

Spatial Localization of *B. cereus* controls coagulation

We hypothesized that initiation of coagulation by bacteria would be regulated by the spatial localization, not the total amount, of bacteria (Fig 1a). In other words, for bacteria that activate coagulation factors, coagulation would only occur when a cluster of bacteria forms. This hypothesis was based on previous experiments with human blood and plasma that showed i) stimuli must exceed a local threshold concentration to initiate coagulation,[1,2] and ii) this threshold response to concentration leads to a spatial threshold response, in which coagulation initiated on a patch of stimulus above, but not below, a threshold size.[3,4]

To test this hypothesis, we compared the clot time of human blood plasma exposed to bacteria dispersed in solution to bacteria clustered on the surface of a microfluidic chamber *Bacillus cereus* (*B. cereus*) spatially localized to a surface cluster rapidly initiated coagulation. However, *B. cereus* dispersed in solution at concentrations of up to 10^7 colony-forming units (CFU) mL^{-1} (Fig 1b). In a second experiment, we used microfluidics[5,6] and micropatterned surfaces to control the spatial distribution of bacteria and to demonstrate that the size of the

cluster, rather than amount of bacteria, can control the rate of initiation of coagulation of human blood plasma. On smaller patches (90 □m) spaced far apart (400 □m), coagulation was slow, initiating on the first patch in 9 min □ 1 with clotting on all the patches in the array in 22 □ 3 min (mean □ S.E.), indicating that the individual, 90 □m patches were below the size necessary to initiate coagulation rapidly (Fig. 1c). However, when the same number of bacteria were patterned closer together to form a large patch, coagulation initiated rapidly in 5 □ 1 min (mean □ S.E.) over the entire patch (Fig. 1d) (p-value < 0.01 in comparison to initiation on the first 90 □m patch, and < 0.005 in comparison to initiation on the entire set of patches).

***B. cereus* initiates coagulation of flowing whole blood**

To test if *B. cereus* would initiate coagulation in the presence of flow, human whole blood was flowed over localized colonies of *B. cereus* in microfluidic channels (Fig. 2). Clusters of bacteria in microfluidic channels were made by encapsulating bacteria in gel microdroplets (GMDs).[7] GMDs consisted of colonies of bacteria and magnetic particles 1 μm in diameter contained in agarose spheres approximately 50 μm in diameter; the magnetic particles allowed the GMDs to be trapped in the microfluidic channels by a magnet incorporated in the device near the channel (Fig. 2a).[8] Clusters of *B. cereus* initiated coagulation of flowing human whole blood in 3–13 min (Fig. 2b,c), whereas coagulation did not occur until 48–59 min in experiments with the control strain of *E. coli* (Fig. 2d, p < 0.001).

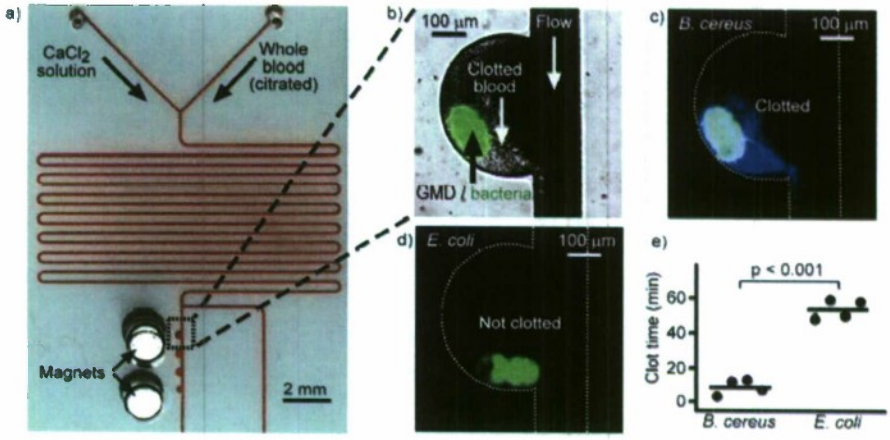

Figure 2. Human whole blood coagulated on spatially localized B. cereus in the presence of flow. (a) A microphotograph shows the microfluidic device used to flow human whole blood over colonies of bacteria. The bacteria were localized in gel microdroplets (GMDs) that also contained magnetic particles. Magnets were used to localize the GMDs in the device. (b) A brightfield image shows coagulation of human whole blood on GMDs containing B. cereus expressing GFP (overlaid green fluorescence). (c-d) Microphotographs of fluorescence show coagulation of human whole blood (blue) on GMDs containing B. cereus (green) (c), but on not E. coli (green) (d). White dashed lines outline the channel walls. Images were taken 11 min after blood was introduced into the device. (e) A graph shows the clot times of flowing whole blood on colonies of B. cereus and E. coli in microfludic devices. Each data point represents an independent experiment.

Clusters of *B. anthracis* initiate coagulation in mice

We used a mouse model to test whether the correlation between clustering of *B. anthracis* and local coagulation was also observed *in vivo*. Mice were injected with *B. anthracis* vegetative bacteria, and then lung, heart, spleen, and liver tissues were harvested quickly (30 or 90 min) after the injection. Rapid harvesting was used to minimize initiation of coagulation by the immune response.[9,10] After harvesting, histological sections of the mouse tissues were scored for the percentage of vessels showing fibrin clots. In the control experiment, two mice were injected with 10^4 bacteria per mouse; we hypothesized that clusters of bacteria would be less likely to form at such a low dose. In these control mice (Fig. 3a), no clusters of bacteria and no fibrin clots were observed in any tissue. Then, two mice were injected with a higher dose of 10^8 bacteria per mouse; we hypothesized that the formation of bacterial clusters would be more likely at this high dose. In the mice receiving 10^8 bacteria, clusters of *B. anthracis* were observed in the microvasculature of the lungs (Fig. 3b), but not in any other organs 30 min after the injection.

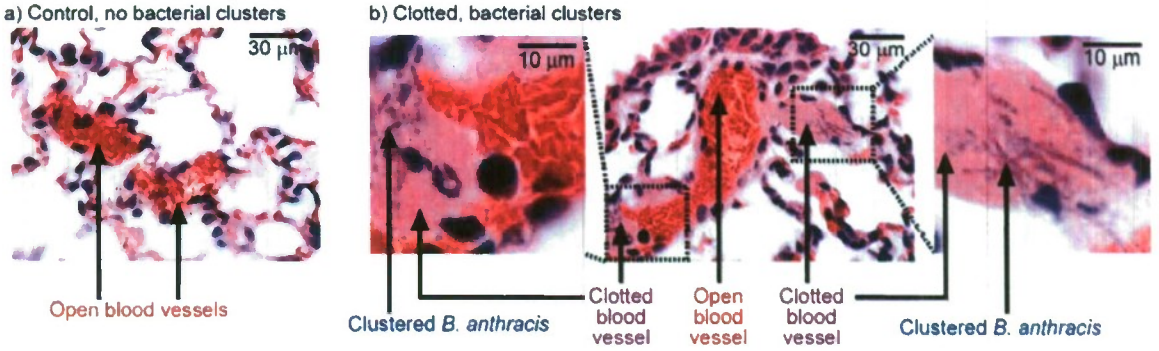

Figure 3. Clusters of B. anthracis rapidly initiate coagulation in mice. (a-b) Hematoxylin and eosin (H&E) stained histological sections of mouse lung. The sections outlined in black were obtained with 100× magnification. (a) Pulmonary vessels from control mice injected with a low dose of bacteria show no clusters and no coagulation. (b) Pulmonary vessels from mice injected with a higher dose of bacteria show clustering of bacteria. Coagulation in vessels (large magenta regions) occurred on clusters of bacteria (chains of rod-like bacteria are seen, blue) within 30 min. Digitally magnified portions of a vessel are shown in images on the left and right.

Confinement regulates initiation of coagulation by tissue factor

Next, we hypothesized that bacteria could also initiate coagulation if sufficiently limited mass transfer caused active factors to accumulate above the local threshold concentration required for coagulation. Confinement—enclosing the source of diffusing molecules within a boundary that these molecules cannot cross—is a simple way to limit mass transfer. First, we tested in general whether confinement could affect the outcome of coagulation, by using microfluidics to confine microparticles carrying a classical stimulus, tissue factor (TF) (Fig. 4). We found that small TF-coated magnetic silica microparticles ("TF-carrying beads") did not initiate clotting of human normal pooled plasma for over 40 min when in a less confining space (160 x 160 μm^2 channels) (Fig. 1*B*) even when the beads were located close to a wall. However, equal-sized or even slightly smaller TF-carrying beads initiated clotting in under 10 min when trapped in a tightly confining space (10 x 10 μm^2 channels) (Fig. 1*C*) (N=5 beads in 2 separate experiments, $p < 0.001$). This result indicates that TF-carrying beads smaller than threshold size did not initiate coagulation in a less confined environment, but did initiate coagulation when they were highly confined in a space with limited diffusion.

Coagulation of human plasma is a complex process that has been shown to exhibit a threshold response (on and off) to the concentration of soluble active coagulation factors such as thrombin.[11] We hypothesized that the observed response to confinement was due to accumulation of soluble active factors, but it was possible that unknown interactions between the plasma and the device also played a role. To exclude this possibility, we tested whether the response to confinement could be predicted by a numerical simulation of TF-initiated blood clotting, using a set of 40 rate equations describing enzyme kinetics and stoichiometric inhibition in blood coagulation without surface interactions[12-14]. We used a simulation with geometry similar to that of the experimental microfluidic device and simulated the response of plasma to small regions, or patches, of 1 nM TF in either 10 μm or 160 μm wide channels (Fig. 5). This simulation was conducted in 2-dimensional space (2D) to reduce computational demands. The clot time was defined as the time at which fibrin reached half of its maximum concentration (i.e., at 4.15 μM fibrin). As predicted, patches of TF initiated the coagulation network quickly (~ 8 min) in confining channels, but not in the less confining channels (> 60 min). This finding agrees with the experimental results (Fig. 4) and confirms that coagulation kinetics and spatial constraints alone are sufficient to achieve the confinement effect.

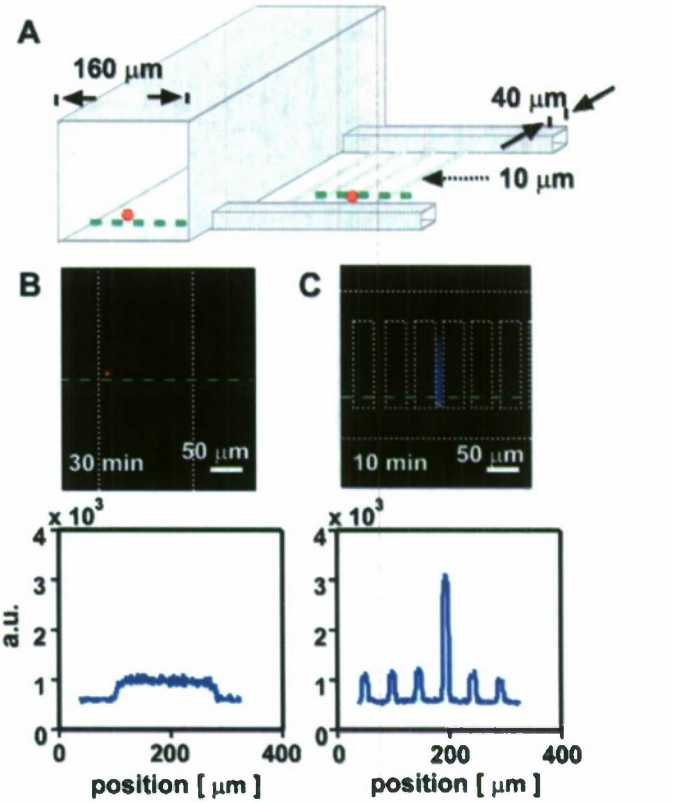

Figure 4. Initiation of blood coagulation by TF-carrying beads is regulated by environmental confinement. (A) A schematic drawing shows the geometry of the experimental device containing channels of different sizes (cross sections of 160 × 160 μm^2, 40 × 40 μm^2, and 10 × 10 μm^2) and TF-carrying beads (Red). (B,C) Initiation of coagulation by TF-carrying beads (red fluorescence) was monitored by using a fluorogenic substrate for thrombin. White dotted lines indicate channel walls of microfluidic device. (B) A representative TF-carrying bead did not initiate coagulation in a less confining channel (160 × 160 μm^2). (C) A representative TF-carrying bead did initiate coagulation (blue) in a more confining channel (10 × 10 μm^2). Linescans of fluorescent intensity along the green dashed line are given below the images.

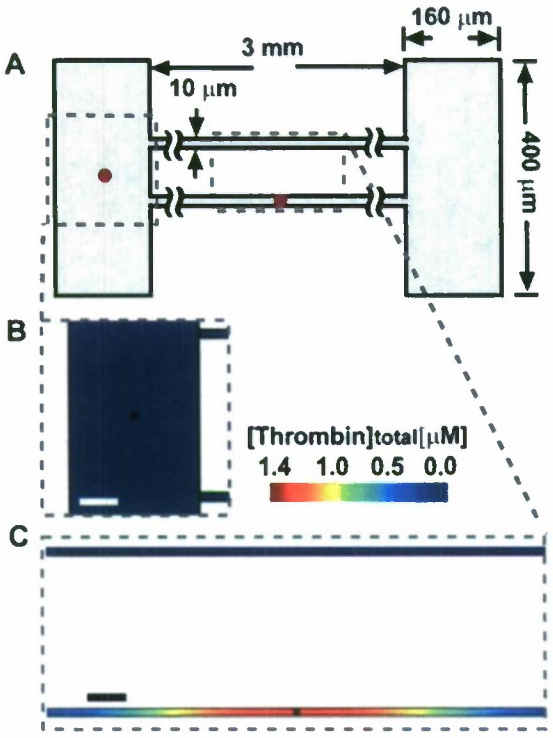

Figure 5. In 2-dimentional simulations of sub-threshold patches of TF (1 nM; radius r = 3 μm) placed in either confining or less confining channels of plasma, clotting initiated only in the confined space. (A) A schematic drawing shows the device design. (B,C) Plots show $[thrombin]_{total}$, the sum of [thrombin] and [meizothrombin], including both free and bound species, at t = 10 min. (B) In less confining (160 μm) channel, no coagulation was initiated at 10 min, and $[thrombin]_{total}$ remained at a low level (blue). (C) In confining space (10 μm) containing a patch, clotting was initiated and $[thrombin]_{total}$ increased to a high concentration (red). No clotting was initiated in the top channel (blue), which did not contain a patch of TF. Scale bars = 50 μm. The red dots in the schematic indicate patches of TF, and they are not drawn to scale.

Confinement regulates initiation of coagulation by bacteria GMDs

Having tested and described initiation of coagulation by TF in confined volumes, we then tested the hypothesis that confinement of bacteria could lead to coagulation of plasma *in vitro*. We tested whether a sub-threshold cluster of *Bacillus cereus* (*B. cereus*) could also initiate coagulation by limiting mass transfer of active factors using confinement. In these experiments, we placed human platelet poor plasma with sub-threshold size gel microdroplets (GMDs) carrying *B. cereus*, "bacteria GMDs", in large microfluidic chambers with diameter of 9 mm and height of 1mm and in small microfluidic channels with dimensions 40 x 40 μm^2 (Fig. 6). In less confining microfluidic chambers, active factors generated by individual bacteria GMDs were constantly removed by diffusion, and bacteria GMDs did not initiate coagulation for over 20 min (Fig. 6*A*); however, placing similarly-sized individual bacteria GMDs in confining microfluidic channels decreased the clot time to less than 10 min (Fig. 6*B*) (N = 3 beads in 3 separate experiments, $p < 0.05$). This result indicates that confining microfluidic channels limit the mass transfer of active factors generated by bacteria GMDs and allow active factors to accumulate locally above threshold concentration to initiate blood coagulation.

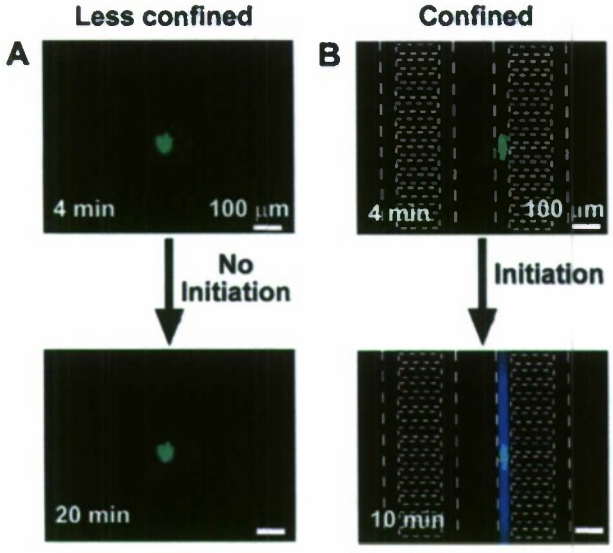

Figure 6. Bacteria gel microdroplets (GMDs) initiate clotting rapidly only when confined. Initiation of coagulation by bacteria GMDs (green fluorescence) was monitored by using a fluorogenic substrate for thrombin. White dotted lines indicate channel walls of microfluidic device. (A) A cluster of *B. cereus* on a GMD did not initiate clotting in a less confining microfluidic chamber (9 mm diameter × 1 mm height) for 20 min. (B) A cluster of *B. cereus* on a GMD did initiate clotting (blue) in a confining channel in 10 min (40 × 40 μm^2 channels).

Chemical Amplification with Threshold

To generate a threshold we decided to use a system with an enzyme, its inhibitor, and its substrate, in which the input is the enzyme and the output is the product of catalysis. A theoretical model was developed to predict in which case one can have a practical threshold. The existence of a practical threshold is generally defined as a big relative difference between the amount of output when the input is slightly below the threshold and that when the input is slightly above threshold. Explicitly, one can use two parameters α and γ to define the existence of practical threshold as

$$(1) \qquad Output\left[Input=(1+\alpha)Threshold\right]-Output\left[Input=(1-\alpha)Threshold\right]\geq\gamma\left(MaxOutput\right)$$

In the model, by letting the enzyme equilibriate with the inhibitor and subsequently allowing the unbound enzyme to catalyze the production of the product, the rate of production of the output is

$$(2) \qquad rate=\frac{k_{cat}E_{available}S_0}{S_0+K_M}$$

$$E_{available}=E_0-\frac{1}{2}\left(E_0+I_0+K_D-\sqrt{-4E_0I_0+\left(E_0+I_0+K_D\right)^2}\right)$$

and a practical threshold exists when

$$(3) \qquad Threshold=I_0\geq K_D\frac{\gamma\left(\alpha\gamma+\gamma-\alpha\right)}{\alpha^2\left(1-\gamma\right)}$$

where E_0, I_0, and S_0 are initial concentration of the enzyme, inhibitor, and substrate, respectively, k_{cat} and K_M are Michaelis-Menten rate constants, K_D is the dissociation constant of the enzyme-inhibitor complex.

To check the validity of the above results, assays were performed with acetylcholinesterase (whose inhibitor is m-isopropyl-2',2',2'-trifluoroacetophenone, with K_D of 6.3 nM as determined by simple inhibitory assays) and thrombin (whose inhibitor is hirudin with K_D of 20 fM[15]). Reaction rates were normalized by the rate of the fastest reaction in the set. Equation (2) was used for theoretical data. Experimental initial rates were calculated from time trace of fluorescence intensity. Indeed, the theoretical model and experimental data agree well (Figure 7).

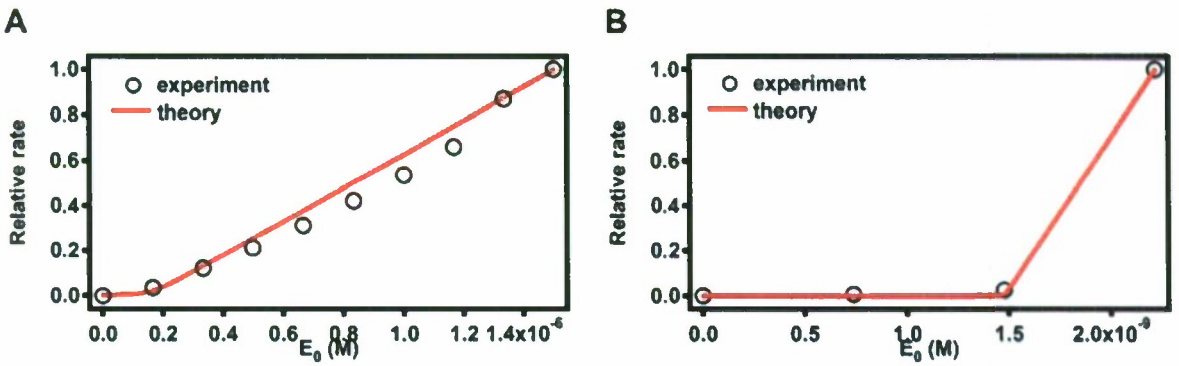

Figure 7. Agreement between theory and experiment for A) acetylcholinesterase/ m-isopropyl-2',2',2'-trifluoroacetophenone (1.7×10^{-7} M) and B) thrombin/hirudin (1.5×10^{-9} M). Substrates for acetylcholinesterase and thrombin were indoxyl acetate (1.3×10^{-5} M) and (Boc-Asp(OBzl)-Pro-Arg-MCA (1.7×10^{-5} M), respectively.

Analog-to-digital Conversion of Chemical Signal with Application for Diagnostics

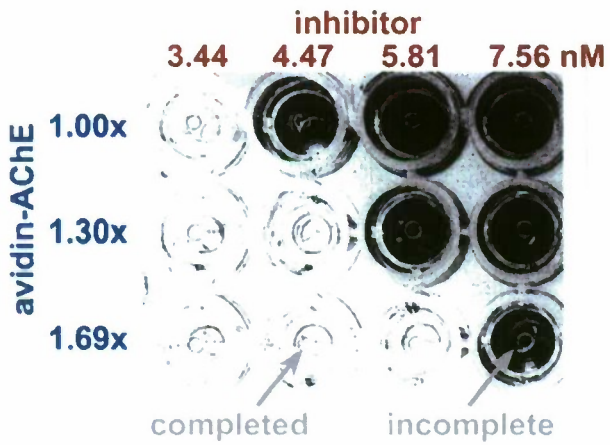

Figure 8. Threshold with AChE (avidin-AChE conjugate) with visual readout. Inhibitor concentration was set up in steps of 1.3 fold. A 1.3-fold increase in enzyme concentration is detected by a step in the position of the threshold (i.e. an increase in the number of completed reactions). The reactions took place in a 96-well plate, and the total volume in each well was 43 μL. Concentrations were final concentrations; the concentration of ths substrate acetylthiocholine was 0.93 mM. The image was taken at 39 minutes with a stereoscope with incident light. The image was subtracted by the image at 151 minutes (when all wells had reacted), and then corrected with Photoshop (contrast+95).

We applied chemical amplification with threshold to converting analog chemical signals (e.g. concentration of a substance) into digital signals (a series of on/off reactions) that describes the analog signal. This conversion was achieved by subjecting the input concentration to different thresholds. From the on/off results of these tests, we can infer quantitative information about the input. A potential use of this technique is quantitation in resource-limited settings where traditional techniques such as absorption or fluorescence require unavailable extra equipment. Particularly, we applied this technique into an immunoassay for cystatin C, a biomarker of kidney function. We used SlipChip[16] as the microfluidic platform for the assay because it

accommodates multistep processing (required for the immunoassay) and multiplexing (required for the analog-digital conversion).[17-19] The chemistry we developed uses acetylcholinesterase (AChE) as the reporter for the immunoassay, a 33-fM inhibitor to set up the threshold,[20] acetylthiocholine as the substrate, and the starch/I^{3-} complex that would react with the product to become clear to produce a visual readout (dark to clear). We first tested this chemistry in well plates (Figure 8). This chemistry allows for visualization of the signal by the naked eyes and recording the results with a consumer's camera. We were able to distinguish 0.64 mg/L cystatin C (normal concentration) from 0.96 mg/L cystatin (stage 3 chronic kidney disease)[21,22] in 5 μL serum as shown in Figure 9. The average difference in the number of incomplete reactions was 3, and the 95%-confidence interval was 0.9-5.1.

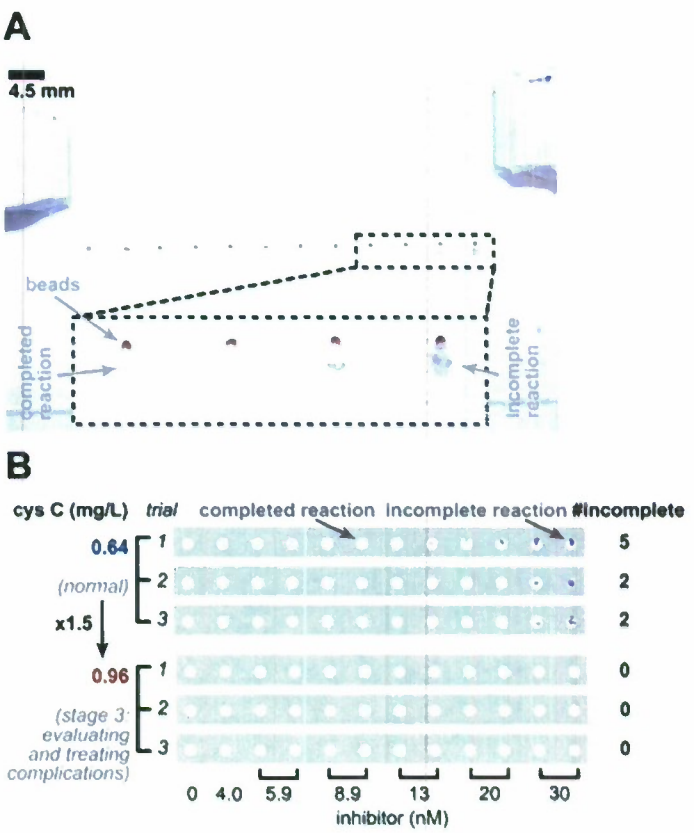

Figure 9. Detection of 1.5 fold change in concentration of cystatin C. (A) Unmodified picture of SlipChip (0.64 mg/L trial 3 at 55 minutes). (B) Distinguishing between 0.64 mg/L cystatin C (normal concentration) and 0.96 mg/L cystatin (stage 3 chronic kidney disease)[21,22] in serum diluted 2 times in PBS buffer (pH 7, with Pluronic F127 1 mg/mL). 5 μL of sample in cystatin C-spiked serum was used for each trial. Each trial required 3 one-hour incubations: binding with the antibodies (one of which bound to beads and the remaining of which bound to biotin) followed by washing, binding with avidin-acetylcholinesterase followed by washing, and reaction with the inhibitor. The concentrations of the inhibitor droplets are shown in the figure, while the concentration of acetylthiocholine in the substrate mixture droplet was 1.0 mM. The pictures were taken after 55 minutes of the reaction (except for 0.96 mg/L cystatin C trial 2 which is presented at 40 min, at which point the reactions had already completed) with a standard digital SLR camera (Canon RebelXT with EFS18-55mm lens). The images were rotated and cropped with ImageJ, then adjusted with Photoshop (level change by setting a spot between wells 6 and 7 to be white, brightness+40, contrast+100), and masked to draw attention to the substrate area with Freehand.

Conclusions

This project has been successful in demonstrating that we can begin to understand the spatiotemporal dynamics of complex reaction networks by using a chemical model of a network that is based on a modular mechanism.

The results presented here demonstrate how local confinement of a small amount of stimulus, such as TF or clot-inducing bacteria, can dramatically alter the outcome of coagulation, a nonlinear reaction network with threshold kinetics. These results demonstrate that a simple physical phenomenon, accumulation of activators due to environmental confinement, can have nontrivial consequences when applied to a reaction system having threshold kinetics. We also demonstrated that we can observe a chemical threshold with an enzyme and an inhibitor. In

ongoing work, we are applying this threshold to detect particles (e.g. bacteria) in microfluidic devices with stochastic confinement. Thresholds abound in physiology, including thresholds seen in blood coagulation[23,24] and activation thresholds in the immune system,[25] so we expect confinement to play a role in many contexts. In ongoing work, we are investigating the use of thresholds for chemical amplification.

Publications supported by this award

Christian J. Kastrup, Matthew K. Runyon, Feng Shen, and Rustem F. Ismagilov, "Modular chemical mechanism predicts spatiotemporal dynamics of initiation in the complex network of hemostasis", *PNAS* **2006** 103:15747-15752

Christian J. Kastrup, Feng Shen, and Rustem F.Ismagilov, "Response to Shape Emerges in a Complex Biochemical Network and Its Simple Chemical Analogue", *Angew. Chem. Int. Ed.* **2007** 46: 3660-3662

Matthew K. Runyon, Bethany L. Johnson-Kerner, Christian J. Kastrup, Thuong G. Van Ha, and Rustem F. Ismagilov, "Propagation of Blood Clotting in the Complex Biochemical Network of Hemostasis Is Described by a Simple Mechanism", *JACS* **2007** 129: 7014-7015

Christian J. Kastrup, Feng Shen, Matthew K. Runyon, and Rustem F.Ismagilov, "Characterization of the Threshold Response of Initiation of Blood Clotting to Stimulus Patch Size", *Biophysical Journal* **2007** 93:2969-2977

Christian J. Kastrup, and Rustem F. Ismagilov, "A physical organic mechanistic approach to understanding the complex reaction network of hemostasis (blood clotting)", *J. Phys.Org. Chem.* **2007** 20:711-715

Matthew K. Runyon, Christian J. Kastrup, Bethany L. Johnson-Kerner, Thuong G, Van Ha, and Rustem F. Ismagilov, "Effects of Shear Rate on Propagation of Blood Clotting Determined Using Microfluidics and Numerical Simulations", *JACS* **2008** 130: 3458-3464

Rebecca R. Pompano, Hung-Wing Li, and Rustem F. Ismagilov, "Rate of mixing controls rate and outcome of autocatalytic processes—theory and microfluidic experiments with chemical reactions and blood coagulation", *Biophysical Journal* **2008** 95: 1531-1543

Feng Shen, Christian J. Kastrup, Ying Liu, and Rustem F. Ismagilov, "Threshold Response of Initiation of Blood Coagulation by Tissue Factor in Patterned Microfluidic Capillaries Is Controlled by Shear Rate ", *Arterioscler. Thromb. Vasc. Biol.* **2008** *published on line.*

Christian J. Kastrup, James Q. Boedicker, Andrei P. Pomerantsev, Mahtab Moayeri, Yao Bian, Rebecca R. Pompano, Timothy R. Kline, Patricia Sylvestre, Feng Shen, Stephen H. Leppla, Wei-Jen Tang and Rustem F. Ismagilov, "Spatial localization of bacteria controls coagulation of human blood by 'quorum acting'", *Nature Chemical Biology* **2008** 4(12): 742-750.

Christian J. Kastrup, Matthew K. Runyon, Elena M. Lucchetta, Jessica M. Price, and Rustem F. Ismagilov, "Using Chemistry and Microfluidics to Understand the Spatial Dynamics of Complex Biological Networks", *Acc. Chem. Res.* **2008** 41:449-558

Feng Shen, Rebecca R. Pompano, Christian J. Kastrup, and Rustem F. Ismagilov, "Confinement Regulates Complex Biochemical Networks: Initiation of Blood Clotting by 'Diffusion Acting'", *Biophysical Journal* **2009** 97: 2137-2145

Meghan E. Vincent, Weishan Liu, Elizabeth B. Haney , and Rustem F. Ismagilov, "Microfluidic stochastic confinement enhances analysis of rare cells by isolating cells and creating high

density environments for control of diffusible signals", *Chem. Soc. Rev.* **2010** 39: 974-984

Feng Shen, Wenbin Du, Jason E. Kreutz, Alice Fok, and Rustem F. Ismagilov, "Digital PCR on a SlipChip", *Lab Chip* **2010** 10:2666-2672

References:

(1) Jesty, J.; Rodriguez, J.; Beltrami, E., "Demonstration of a threshold response in a proteolytic feedback system: Control of the autoactivation of factor XII" **2005**, *34*, 71-79.

(2) vantVeer, C.; Mann, K. G., "Regulation of tissue factor initiated thrombin generation by the stoichiometric inhibitors tissue factor pathway inhibitor, antithrombin-III, and heparin cofactor-II" **1997**, *272*, 4367-4377.

(3) Kastrup, C. J.; Runyon, M. K.; Shen, F.; Ismagilov, R. F., "Modular chemical mechanism predicts spatiotemporal dynamics of initiation in the complex network of hemostasis" *Proc. Nat. Acad. Sci. USA* **2006**, *103*, 15747-15752.

(4) Kastrup, C. J.; Shen, F.; Runyon, M. K.; Ismagilov, R. F., "Characterization of the threshold response of initiation of blood clotting to stimulus patch size" *Biophys. J.* **2007**, *93*, 2969-2977.

(5) Weibel, D. B.; DiLuzio, W. R.; Whitesides, G. M., "Microfabrication meets microbiology" **2007**, *5*, 209-218.

(6) Whitesides, G. M.; Ostuni, E.; Takayama, S.; Jiang, X. Y.; Ingber, D. E., "Soft lithography in biology and biochemistry" **2001**, *3*, 335-373.

(7) Weaver, J. C.; Williams, G. B.; Klibanov, A.; Demain, A. L., "Gel Microdroplets - Rapid Detection and Enumeration of Individual Microorganisms by Their Metabolic-Activity" **1988**, *6*, 1084-1089.

(8) Siegel, A. C.; Shevkoplyas, S. S.; Weibel, D. B.; Bruzewicz, D. A.; Martinez, A. W.; Whitesides, G. M., "Cofabrication of electromagnets and microfluldic systems in poly(dimethylsiloxane)" **2006**, *45*, 6877-6882.

(9) Opal, S. M.; Esmon, C. T., "Bench-to-bedside review: Functional relationships between coagulation and the innate immune response and their respective roles in the pathogenesis of sepsis" **2003**, *7*, 23-38.

(10) Pawlinski, R.; Pedersen, B.; Kehrle, B.; Aird, W. C.; Frank, R. D.; Guha, M.; Mackman, N., "Regulation of tissue factor and inflammatory mediators by Egr-1 in a mouse endotoxemia model" **2003**, *101*, 3940-3947.

(11) Pompano, R. R.; Li, H. W.; Ismagilov, R. F., "Rate of mixing controls rate and outcome of autocatalytic processes: Theory and microfluidic experiments with chemical reactions and blood coagulation" *Biophys. J.* **2008**, *95*, 1531-1543.

(12) Hockin, M. F.; Jones, K. C.; Everse, S. J.; Mann, K. G., "A model for the stoichiometric regulation of blood coagulation" *J. Biol. Chem.* **2002**, *277*, 18322-18333.

(13) Kogan, A. E.; Kardakov, D. V.; Khanin, M. A., "Analysis of the activated partial thromboplastin time test using mathematical modeling" *Thromb. Res.* **2001**, *101*, 299-310.

(14) Kastrup, C. J.; Boedicker, J. Q.; Pomerantsev, A. P.; Moayeri, M.; Bian, Y.; Pompano, R. R.; Kline, T. R.; Sylvestre, P.; Shen, F.; Leppla, S. H.; Tang, W.; Ismagilov, R. F., "Spatial Localization of Bacteria Controls Coagulation of Human Blood by "Quorum Acting"" *Nat. Chem. Biol.* **2008**, *4*, 742-750.

(15) Stone, S. R.; Hofsteenge, J., "Kinetics of the Inhibition of Thrombin by Hirudin" *Biochemistry* **1986**, *25*, 4622-4628.

(16) Du, W.; Li, L.; Nichols, K. P.; Ismagilov, R. F., "SlipChip" *Lab Chip* **2009**, *8*, 2286-2292.
(17) Liu, W.; Chen, D.; Du, W.; Nichols, K. P.; Ismagilov, R. F., "SlipChip for immunoassays in nanoliter volumes" *Anal. Chem.* **2010**, *82*, 3276-3282.
(18) Shen, F.; Du, W.; Davydova, E. K.; Karymov, M. A.; Pandey, J.; Ismagilov, R. F., "Nanoliter multiplexed PCR arrays on a SlipChip" *Anal. Chem.* **2010**, *82*, 4606-4612.
(19) Shen, F.; Davydova, E. K.; Du, W.; Kreutz, J. E.; Piepenburg, O.; Ismagilov, R. F., "Digital Isothermal Quantification of Nucleic Acids via Simultaneous Chemical Initiation of Recombinase Polymerase Amplification Reactions on SlipChip" **2011**, *83*, 3533-3540.
(20) Krasiński, A.; Radić, Z.; Manetsch, R.; Raushel, J.; Taylor, P.; Sharpless, K. B.; Kolb, H. C., "In Situ Selection of Lead Compounds by Click Chemistry: Target-Guided Optimization of Acetylcholinesterase Inhibitors" **2005**, *127*, 6686-6692.
(21) Levey, A. S.; Coresh, J.; Balk, E.; Kausz, A. T.; Levin, A.; Steffes, M. W.; Hogg, R. J.; Perrone, R. D.; Lau, J.; Eknoyan, G., "National kidney foundation practice guidelines for chronic kidney disease: Evaluation, classification, and stratification" **2003**, *139*, 137-147.
(22) Stevens, L. A.; Coresh, J.; Schmid, C. H.; Feldman, H. I.; Froissart, M.; Kusek, J.; Rossert, J.; Van Lente, F.; Bruce, R. D., III; Zhang, Y.; Greene, T.; Levey, A. S., "Estimating GFR using serum cystatin C alone and in combination with serum creatinine: A pooled analysis of 3,418 individuals with CKD" **2008**, *51*, 395-406.
(23) Jesty, J.; Beltrami, E., "Positive feedbacks of coagulation - Their role in threshold regulation" *Arterioscler. Thromb. Vasc. Biol.* **2005**, *25*, 2463-2469.
(24) Mann, K. G.; Brummel, K.; Butenas, S., "What is all that thrombin for?" *J. Thromb. Haemost.* **2003**, *1*, 1504-1514.
(25) Grossman, Z.; Paul, W. E., "Adaptive Cellular Interactions in the Immune-System - the Tunable Activation Threshold and the Significance of Subthreshold Responses" *Proc. Natl. Acad. Sci. U. S. A.* **1992**, *89*, 10365-10369.